

# NUMERICAL SIMULATION OF PULSATING FLOW IN THREE-DIMENSIONAL S-ARTERY WITH TAPERED ANGLE

Rui Ding<sup>1</sup>, Xiaoping Chen<sup>1</sup>, Qing Wang<sup>2</sup> and Yong Zhang<sup>1</sup>

## ABSTRACT

The pulsating flow in S-artery with tapered angle is studied with finite element method (FEM). Numerical simulation for the pulsating flow in S-artery with tapered angle and no tapered, namely the case of the equal cross section under the same boundary conditions is performed. The results showed that the taper has important influence of hemodynamics in S-artery. The visualization of pulsating blood flow in S-artery reveals that the second flow in the tapered blood vessel is larger, more complex than that in the equal cross section; the vorticity, the maximum and the change of pressure and wall shear stress (WSS) in the tapered blood vessel are also larger than that in the equal cross section. It shows that the influence of taper in S-artery can not be neglected.

**Key words:** Tapered angle, S-shape Artery, Pulsating flow

## 1. INTRODUCTION

Blood flow problems have been studied so many years in the fields of biomechanics, medical science, biology, biomedical engineering etc. Now many studies focused on the geometric model of straight round pipe, aortic arch [5], S-shape artery [2]. The geometric model with the taper angle are almost the straight pipe [1] or the pipe curved by 90°, and so on [3, 4]. As we know, there are no any open reports on the case of the more complicated numerical simulation for the S-artery with tapered angle.

Here we realized the numerical simulation and visualization for the 3-dimensional pulsating flow in S-shaped arteries. By use of FEM, we compute two geometric models, one has a one degree taper angle and the other has no taper. the changes of pressure, velocity, vorticity and the wall shear stress (WSS) in different conditions are obtained. The results showed that the taper has important influence of pulsating flow in S-artery.

## 2. THEORETICAL MODEL

The anatomy and physiology of artery shows that the taper angle of blood vessel is about one degree. The geometric model is shown in Fig. 1, where the curvature radius of the curved artery  $R = 35\text{mm}$ , the inlet flow straight length is 30 mm, and the outlet straight length is 30mm, The taper angle from inlet to outlet in S-artery is one degree; where the inlet diameter  $\Phi_1$  is 25.48mm, the diameter of the tip cross section in the bending flexure  $AA'$  is 24.96mm, while the diameter of the end cross section  $EE'$  is 23.04mm, and the diameter in the outlet section  $\Phi_2$  is 22.52mm, In order to compare with the model of no tapered angle, suppose that the diameter of the equal cross section in the curved S-artery without tapered angle is 24mm and the length of the blood vessel is equal to that of the case with tapered angle.

The following important hypothesis will be used in the rest of the paper: (1) The S-artery is a rigid pipe with tapered angle; (2) The blood vessel is incompressible, homogeneous and Newtonian fluid; (3) The motion of blood in vessels is three -dimensional and unsteady laminar flow.

1. School of Mathematical Science, Suzhou University, Suzhou 215006, China, E-mail: rayting@pub.sz.jsinfo.net

2. Suzhou University, Affiliated Pediatrical Hospital, Suzhou 215003, China, E-mail: edna\_wq@sina.com.cn

In accordance with the above hypothesis, the governing equation of blood flow in the Cartesian coordinate system can be stated as follows, namely Navier-Stokes equation:

$$\frac{\partial \vec{V}}{\partial t} + (\vec{V} \cdot \nabla) \vec{V} = -\frac{1}{\rho} \nabla P + \frac{\mu}{\rho} \nabla^2 \vec{V}, \quad (1)$$

Where  $\rho$  is the blood density, unit  $kg/m^3$ ;  $u, v, w$  express the velocity component of  $\vec{V}$  in the  $X, Y, Z$  direction respectively, unit  $m/s$ .  $P$  is the pressure of the flow field unit  $Pa$  and  $\mu$  is the blood viscosity coefficient with unit  $kg/m \cdot s$ .

The blood vessel is incompressible, thus the mass conservation equation is satisfied, i.e., the continuity equation:

$$\nabla \cdot \vec{V} = 0, \quad (2)$$

The boundary conditions are as follow:

(1) No-slip condition on the wall:  $\vec{V} = 0$ ; (2) The inlet velocity condition: let the cardiac period  $T$  be 0.8s, where the systole is 0.3s and the diastole is 0.5s; there is no radial velocity at the inlet, and the average velocity of the inlet blood stream of the S-shape curved artery see Figure 2; (3) The outlet stress condition at the exit: open boundary, so normal stress  $f = 0$ .

Now we turn to the initial conditions. Let the initial value of all dynamics parameters be 0 and suppose the blood density  $\rho = 1.05 \times 10^3 kg/m^3$ . Furthermore, let the blood viscosity coefficient  $\mu$  be  $0.0035 kg/m \cdot s$  and the peak value of the inlet velocity  $V_{max}$  is  $1.127 m/s$ . By the above conditions, we have:

$$R_e = \Phi_1 \cdot V_{max} \rho / (2\mu) = 4307; \text{ Womersley } \alpha = \Phi_1 \sqrt{2\pi\mu/T\rho} / 2 = 65.$$

Numerical computations are carried out by FEM using Lagrange elements over a tetrahedral mesh. In the process of partition, in order to obtain the accurate pressure and velocity distribution at the curved part, we need to subdivide the grids to improve the calculation accuracy. See Fig. 3 for a partition mesh. In order to compute the dynamic parameters such as velocity and pressure, the time step is 0.01s. Since the blood flow is unsteady and may cause clearly errors in the first period, we compute the three periods to get the stable and more accuracy solutions.

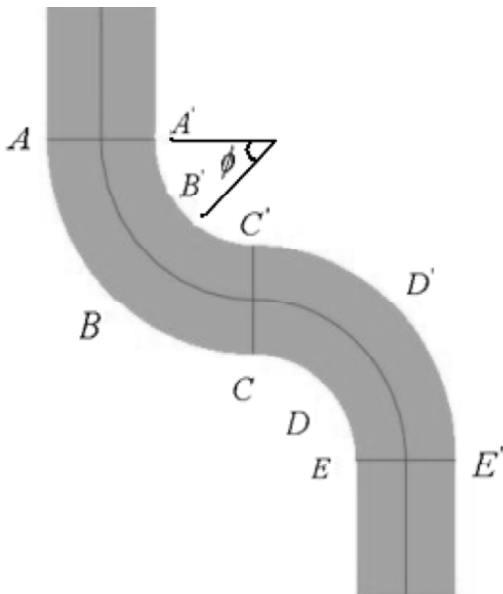


Figure 1: Geometric Model

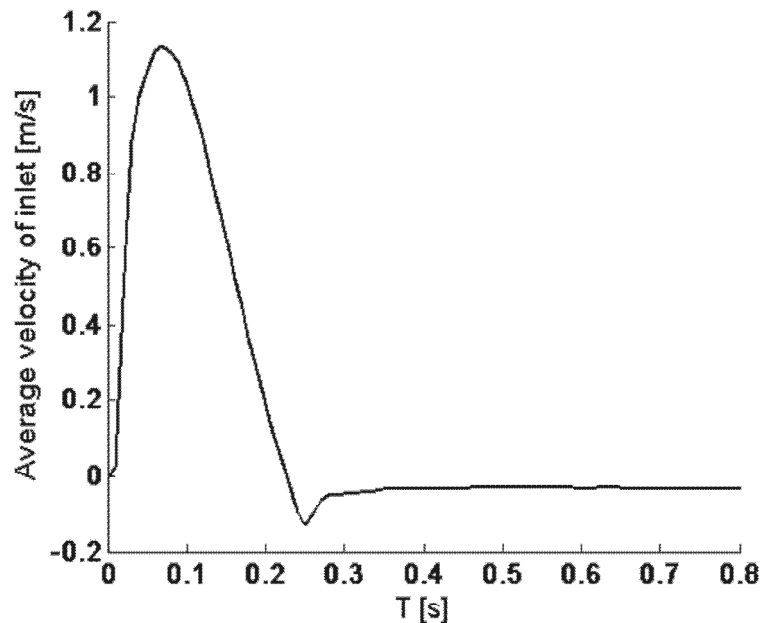


Figure 2: The Average Velocity of Inlet

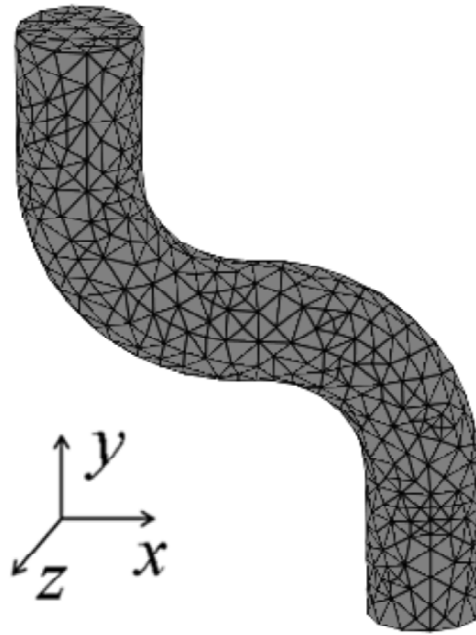


Figure 3: Partition Mesh

### 3. VISUALIZATION COMPUTING

Let some cross sections be  $AA'$ ,  $BB'$ ,  $CC'$ ,  $DD'$ ,  $EE'$ , whose angle are  $0^\circ$ ,  $45^\circ$ ,  $90^\circ$ ,  $135^\circ$ ,  $180^\circ$  respectively.  $AA'$  and  $BB'$  are the inlet cross section and middle cross section of the inlet curved pipe respectively; and  $CC'$  is the junction surface of the inlet pipe and outlet pipe, while  $DD'$  and  $EE'$  are the middle cross section and the outlet cross section of the outlet curved pipe respectively.

In order to analyze the effect of tapered angle on the pulsating flow more precisely, we put the graphs of these two cases together. Here we choose some typical times, namely 0.05s, 0.23s, 0.3s, 0.7s (From Figs. 4 - 12, the upper line is the model without tapered angle and the lower line is the model with tapered angle). Fig 4 and 5 show the pressure and velocity distribution of the longitudinal section at different times, respectively; Figs. 6-8 shows the  $Y$ -Axis velocity distribution of the  $BB'$ ,  $CC'$ ,  $DD'$  cross section at different times; Figs. 9-11 respectively show the pressure distribution of the  $BB'$ ,  $CC'$ ,  $DD'$  sections at different times; Fig 12 shows the vorticity distribution at different times in one period, respectively; Figs. 13-16 depicted the wall shear stress(WSS) distributions at certain locations of the curved segments in one period; E.g., like points  $B$  and  $B'$ , Taper case: real line with triangle is WSS at point  $B$ ; dashed line with circle is WSS at point  $B'$ ; No taper case(equal cross section): real line with star is WSS at point  $B$ ; dashed line with square is WSS at point  $B'$ .

The figure of the inlet average velocity indicates that the inlet velocity increases quickly at the contraction and acceleration period. The maximal axial velocity occurs at the inner bend after the blood flows into the inlet curved part of the pipe. This shows that the flow is in the potential flow state because of the dominant effect of inertia. Then  $v_{\max}$  move from the inner bend into the outer bend along with the central line until the maximal resultant velocity vector arrives at the beginning curved region of the outlet, see Fig. 5. Figs. 6 and 8 indicate that at the contraction and deceleration period, reflow arises gradually at the inner bend of the inlet curved pipe and moves to the curved part of the pipe, while at the relative stable period of relaxation, reflow occupies the entire blood vessel.

Fig. 7 reveals that the second flow of the downstream in the curved blood vessel is more intensive than that of the upstream. Comparing the tapered second flow with the one of the no taper, we can see that the second flow of the tapered pipe is more complicated and intensive, which indicates that the taper has an important effect on the second flow.

Figs. 4, 9, 10 and 11 demonstrates that at the contraction period (systole), the pressure on the outer bend is stronger than that on the inner bend because of the effect of the centrifugal force; while at the period of relaxation (diastole), the pressure value of the outer bend is close to the inner bend and the value in tapered S-shape artery is

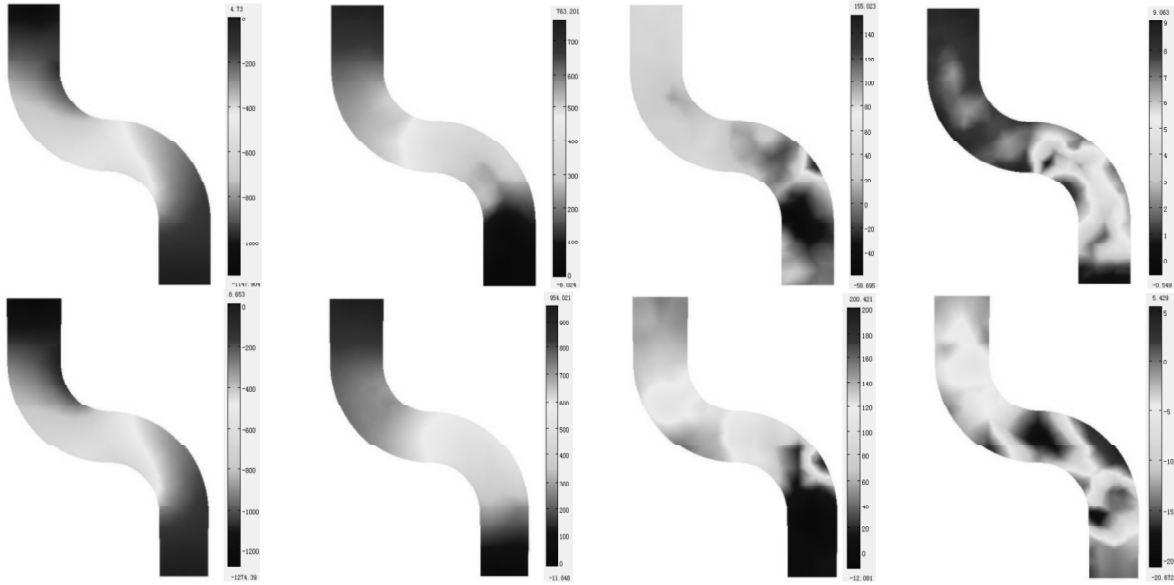


Figure 4: The Pressure Distribution of the Longitudinal Section at Different Times

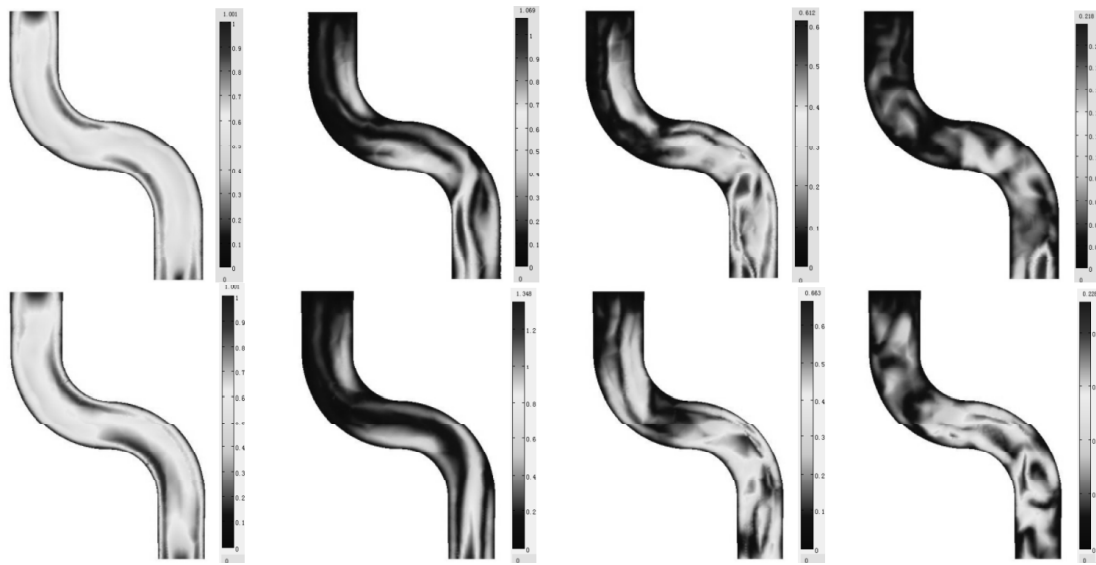


Figure 5: The Velocity Distribution of the Longitudinal Section at Different Times

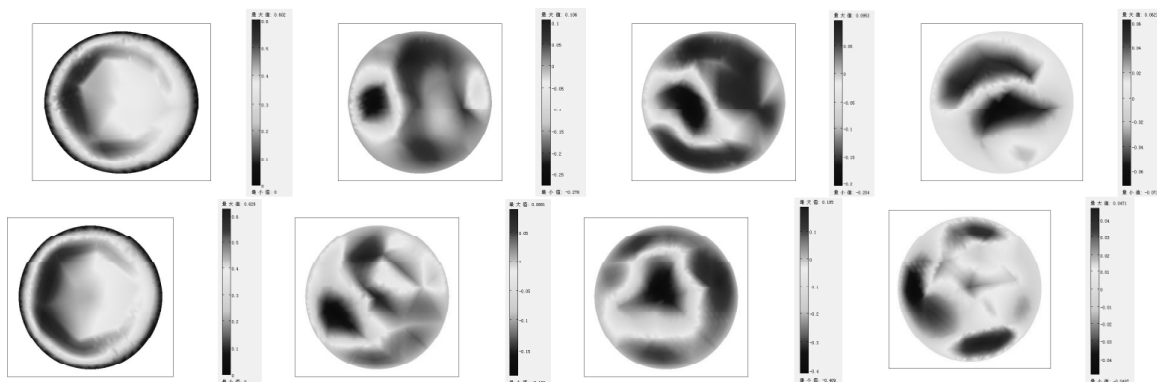


Figure 6: The Y-Axis Velocity Distribution of the  $BB'$  Sections at Different Times

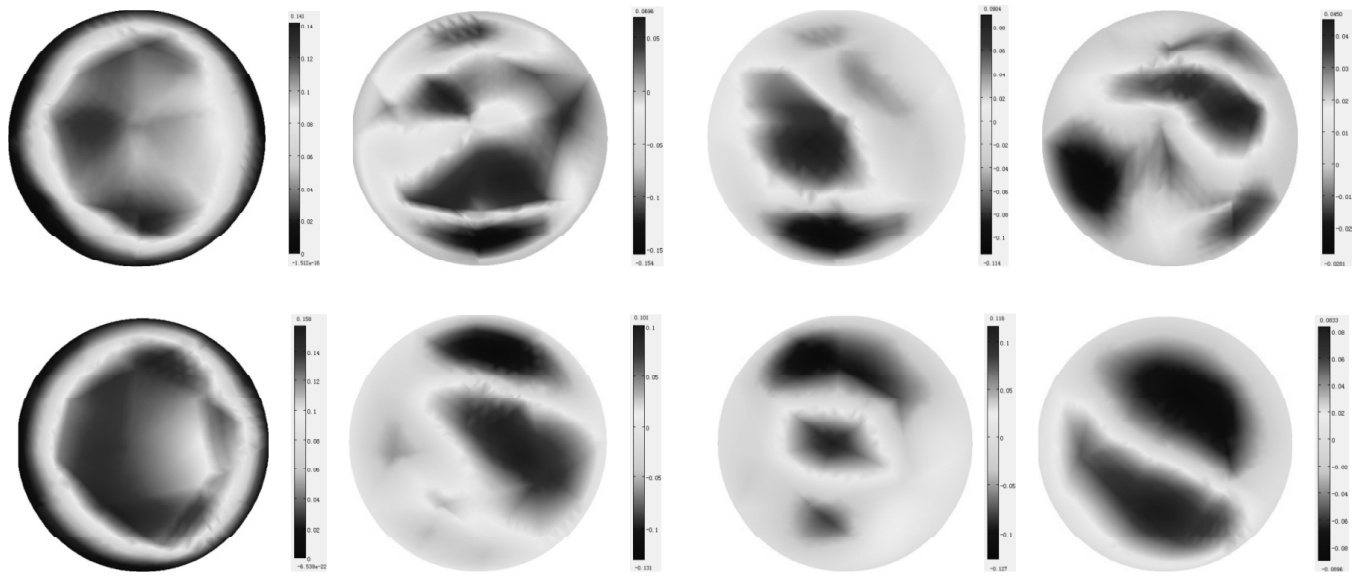


Figure 7: The Y-Axis Velocity Distribution of the CC' Sections at Different Times

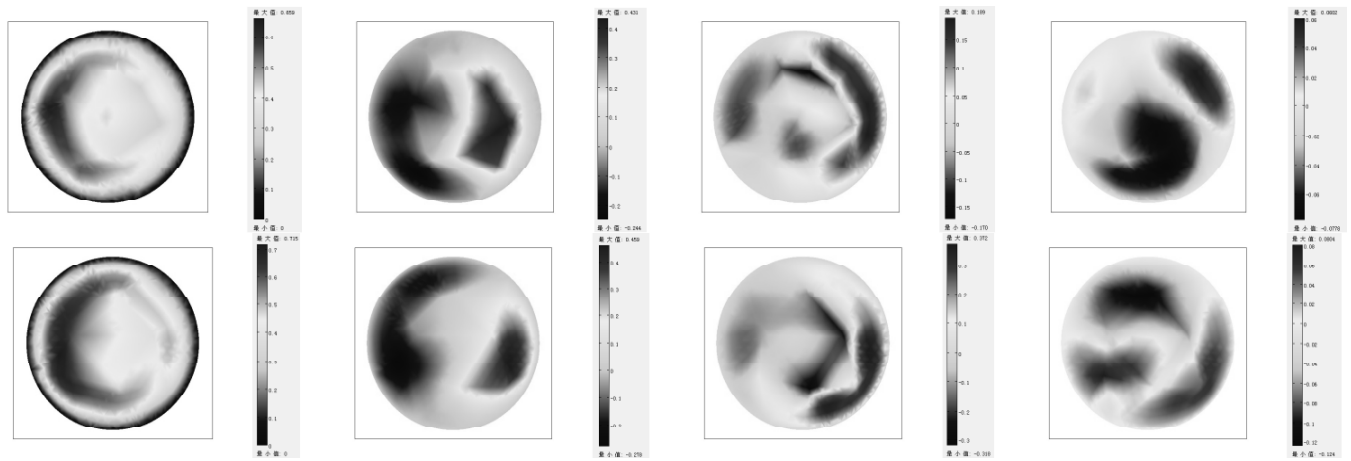


Figure 8: The Y-Axis Velocity Distribution of the DD' Sections at Different Times

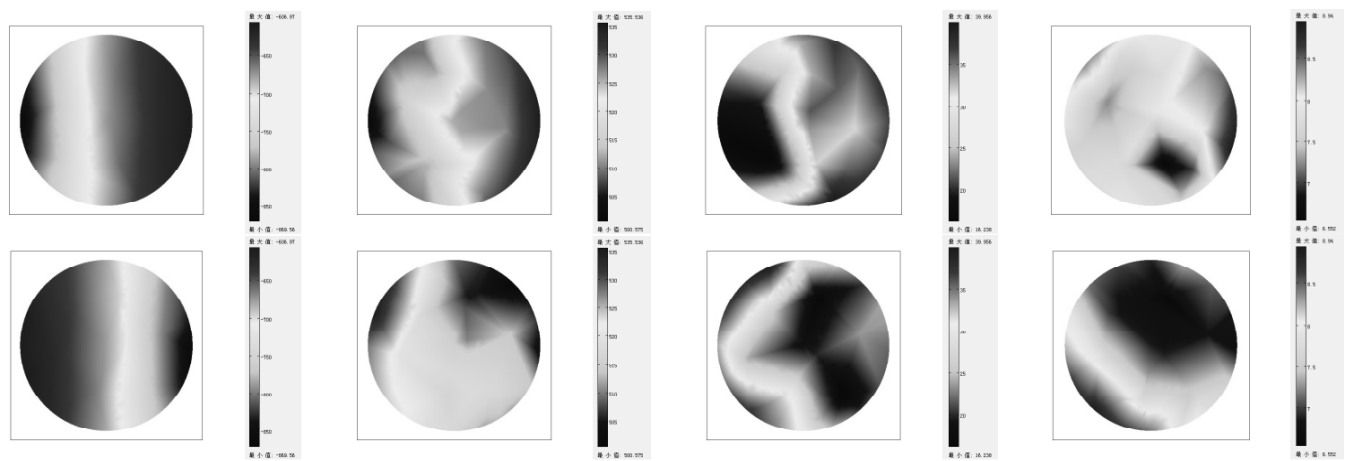


Figure 9: The Pressure Distribution of the BB' Section at Different Times

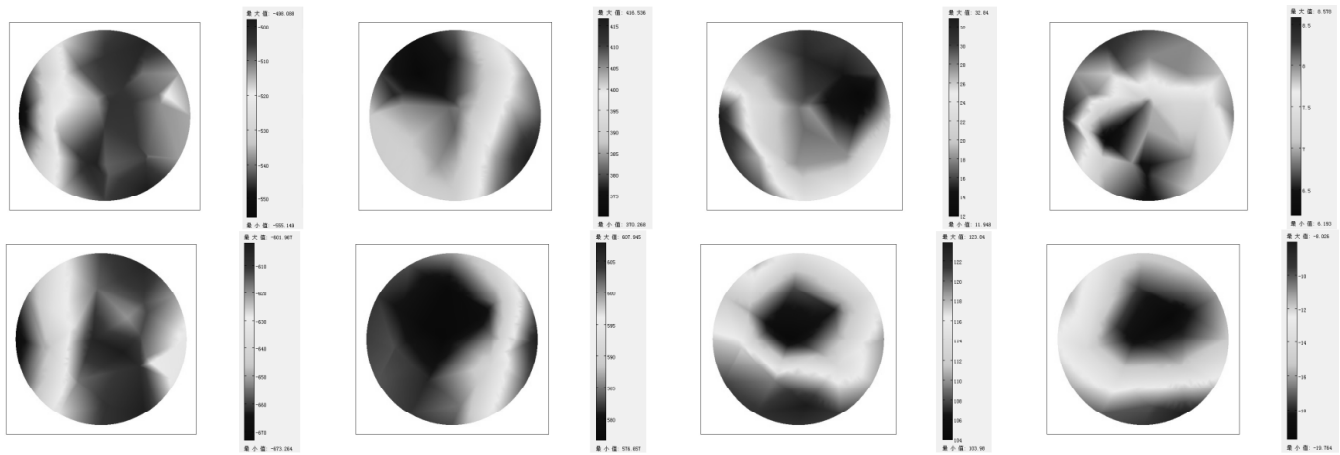


Figure 10: The Pressure Distribution of the CC' Section at Different Times

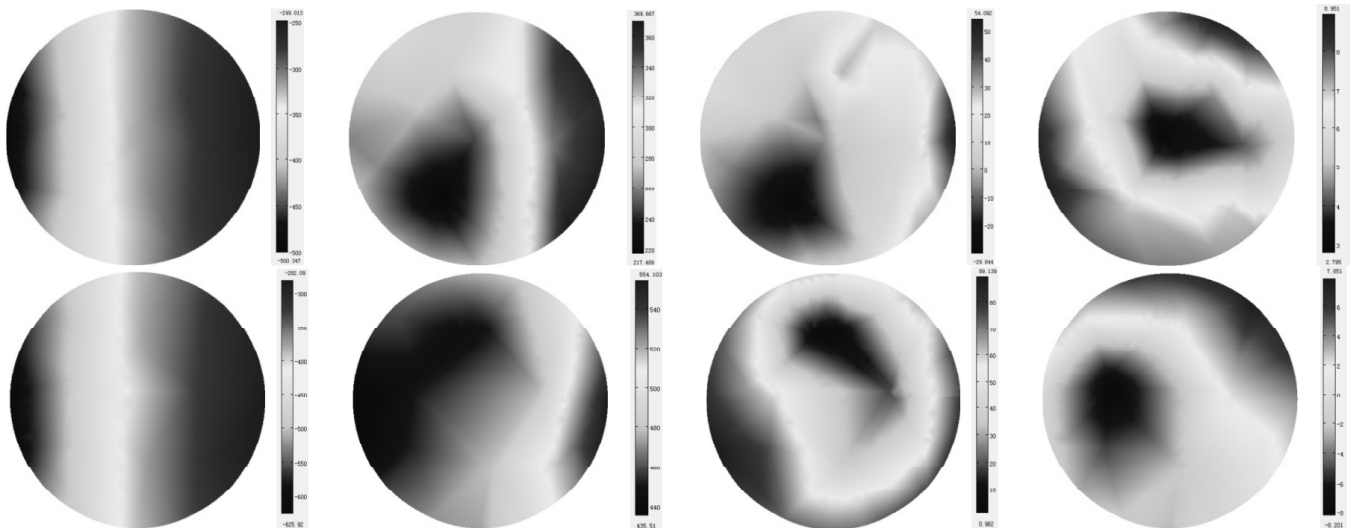


Figure 11: The Pressure Distribution of the DD' Section at Different Times

larger than that in the equal cross section. As a result, the second flow in the tapered blood vessel is larger than that in the equal cross section.

Fig. 12 indicates that at the beginning of the contraction period (systole), the blood flow of the S-shape vessel is similar to the Poiseuille of the long straight vessel. However, the peak value of the velocity declines to the inside of the S-shape artery as a result of the effect of the taper and curvature. At the times except  $t = 0.05s$ , boundary layer separation emerges in the blood flow field, that is, second flow. At time  $t = 0.23s$ , the second flow at the offside of the outlet is much serious. Consequently, stenosis comes into being more frequently. Comparing the blood vessel of the tapered S-shape with that of the equal cross section, it is easily to see that the vorticity distribution in the tapered curved vessel is more complicated.

From Figs 13 to 16, the distributions of the wall shear stress at certain positions of the S-shape artery are shown. It can be seen that these diagrams are similar to each other and they increase or decrease along with the inlet velocity. At the contraction period, the wall shear stress is larger because of the shear rate at the near wall. On the other hand, at the end of the relative calm period of deceleration (diastole), the value of wall shear stress is smaller, as well as its variation. Furthermore, both the tapered and no tapered S-shape artery arrive at the maximal and minimal value of wall shear stress at the same time. But the maximal value and the variation value of the tapered wall shear stress are larger than that of the equal cross section.

4. CONCLUSIONS

The tapered and no tapered S-shape artery are studied in this paper. The results showed that the blood flow in the curved S-shape artery presents characteristics such as complicated reflow, second flow, intensive pressure and wall shear stress variations by comparing tapered and no tapered pulsating flow in the S-shape artery. Moreover, it can be easily to see that there is much difference between the tapered and the no tapered S-shape vessel. In fact, the blood vessel is always tapered, thus considering tapered blood vessel is closer to the practical situation. In a word, the shape and the diameter variation of the blood vessel should not be negligent in the study of pulsating flow.

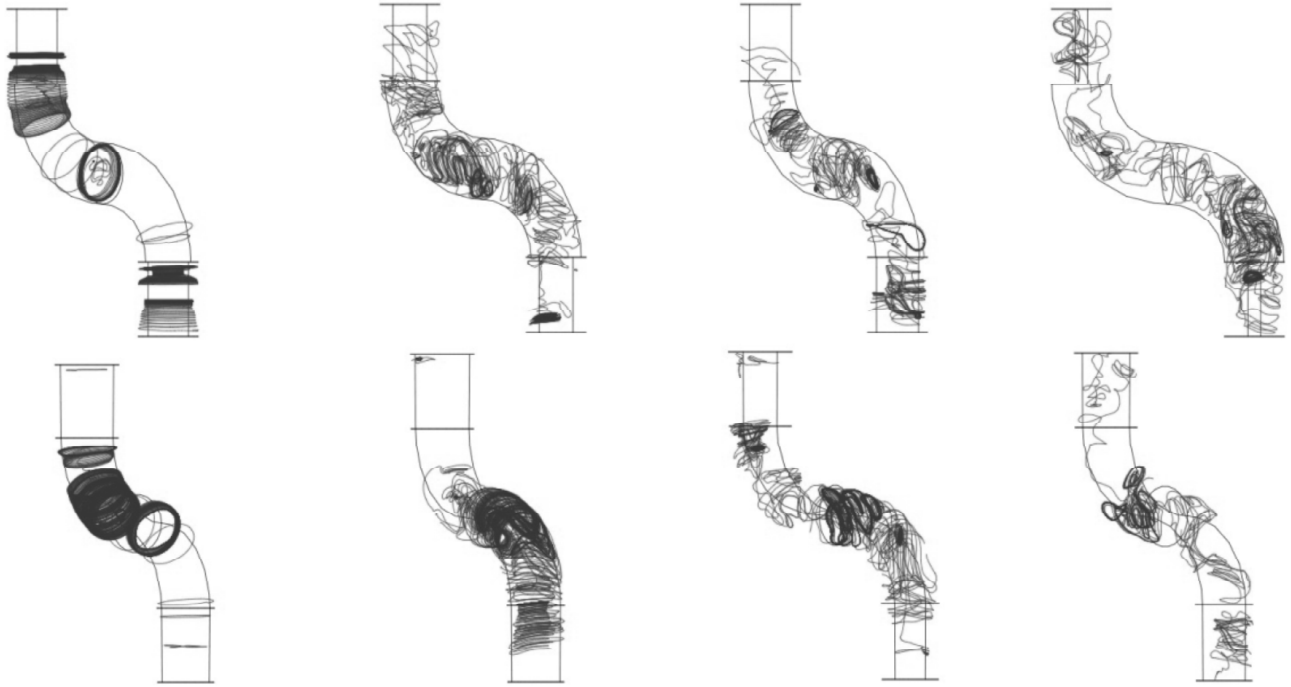


Figure 12: The Vorticity Distribution at Different Times in One Cycle

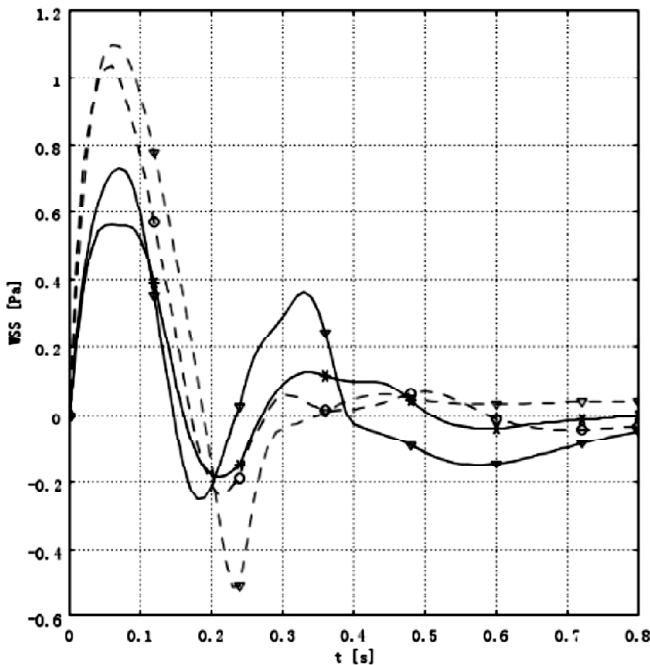


Figure 13: The Wall Shear Stress (WSS) Distributions at B and B'

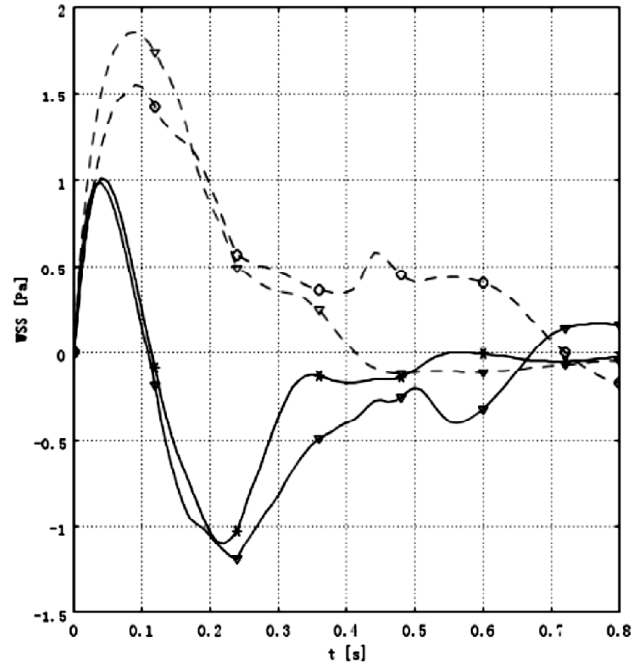


Figure 14: The Wall Shear Stress (WSS) Distributions at C and C'

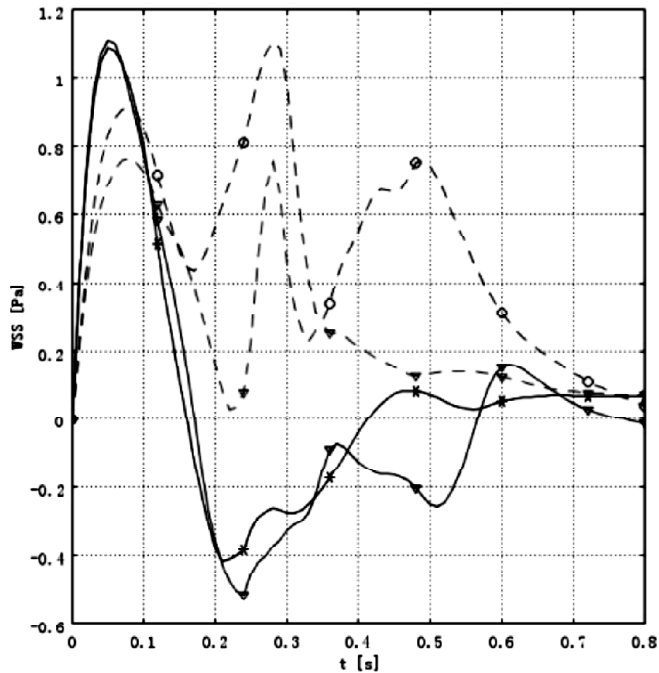


Figure 15: The Wall Shear Stress (WSS) Distributions at  $D$  and  $D'$

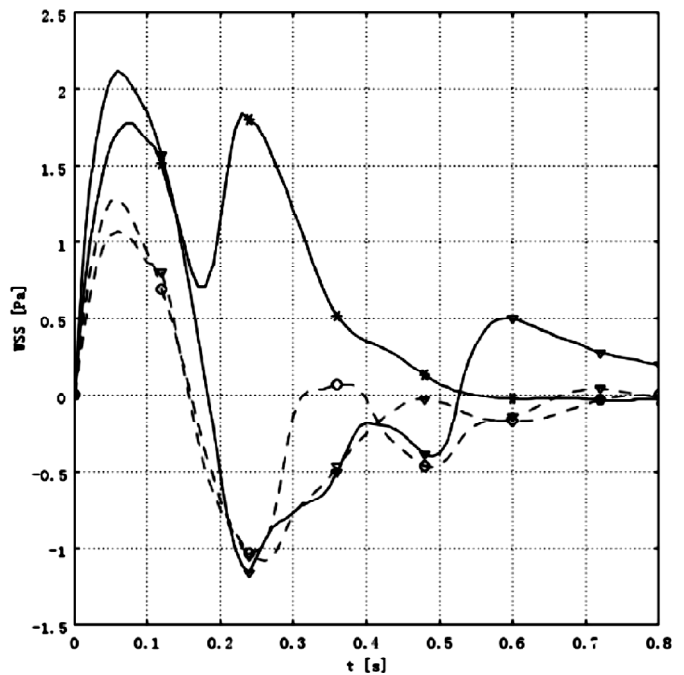


Figure 16: The Wall Shear Stress (WSS) Distributions at  $E$  and  $E'$

### Acknowledgement

This project was supported by the National Natural Science Foundation of China under Grant No.10201026, No.10672111.

### References

- [1] Qiu, L., Fan, Y. F. and Dong, B. C., "The Numerical Simulation of Pulsation Flow in a Tapered Blood Vessel," *Journal of Biomechanics*, **4**, 558-561, (2004).
- [2] Qiao, A. K., Guo, X. L., Wu, S. G., Zeng, Y. J. and Xu, X. H., "Numerical Study of Nonlinear Pulsatile Flow in S-shaped Curved Arteries," *Medical Engineering & Physics*, **26**, 545-552, (2004).
- [3] Wan, D. W., "Three-dimensional Numerical Simulation of Hemodynamics in Human Aortic Arch," *Journal of Medical Biomechanics*, **4**, 279-283, (2008).
- [4] Yang, J. Y., Jin, Y. Z., "The Effects of Taper on the Pulsatile Blood Flow in Aortic Arch," *Journal of Zhejiang Sci-Tech University*, **4**, 470-473, (2008).
- [5] Qiao, A. K., Liu, Y. J. and Wu, S. G., "Numerical Analysis of Hemodynamics in Curved Arteries," *Chinese Journal of Computational Mechanics*, **20**, 142-150, (2003).